American Journal of Physical Anthropology

'Missing perikymata' – fact or fiction? A study on chimpanzee (Pan troglodytes verus) canines

Journal:	*American Journal of Physical Anthropology*
Manuscript ID:	Draft
Wiley - Manuscript type:	Research Article
Date Submitted by the Author:	n/a
Complete List of Authors:	Kierdorf, Horst; University of Hildesheim, Department of Biology Witzel, Carsten; University of Hildesheim, Department of Biology Kierdorf, Uwe; University of Hildesheim, Department of Biology Skinner, Matthew; University of Kent, School of Anthropology and Conservation Skinner, Mark; University of York, Department of Archaeology
Key Words:	enamel, hypoplastic defects, crown growth, striae of Retzius

‘Missing perikymata’ – fact or fiction? A study on chimpanzee (*Pan troglodytes verus*) canines

Horst Kierdorf[1*], Carsten Witzel[1], Uwe Kierdorf[1], Matthew M. Skinner[2,3], and Mark F. Skinner[4]

[1]*Department of Biology, University of Hildesheim, Marienburger Platz 22, 31141 Hildesheim, Germany*

[2]*School of Anthropology and Conservation, University of Kent, CT2 7NR, Canterbury, UK*

[3]*Department of Human Evolution, Max Planck Institute for Evolutionary Anthropology, Deutscher Platz 6, 04103 Leipzig, Germany*

[4]*Department of Archaeology, King's Manor, University of York, YO1 7EP, York, UK*

20 text pages; 1 table, 5 figures

Running headline: Missing perikymata in chimpanzee canines ?

KEY WORDS: Enamel, hypoplastic defects, crown growth, striae of Retzius

*Correspondence to: Horst Kierdorf, Department of Biology, University of Hildesheim, Marienburger Platz 22, 31141 Hildesheim. E-mail: kierdorf@uni-hildesheim.de

ABSTRACT

Recently, a lower than expected number of perikymata between repetitive furrow-type hypoplastic defects has been reported in chimpanzee canines from the Fongoli site, Senegal (Skinner and Pruetz 2012, AJPA 149:468-482). Based on an observation in a localized enamel fracture surface of a canine of a chimpanzee from the Taï Forest (Ivory Coast), these authors inferred that a non-emergence of striae of Retzius could be the cause for the 'missing perikymata' phenomenon in the Fongoli chimpanzees. To check this inference, we analyzed the structure of outer enamel in three chimpanzee canines. Our analysis of the specimen upon which Skinner and Pruetz (2012) had made their original observation does not support their hypothesis. We demonstrate that the enamel morphology described by them is not caused by a non-emergence of striae of Retzius but can be attributed to structural variations in outer enamel that result in a differential fracture behavior. While rejecting the presumed existence of non-emergent striae of Retzius, our study provided evidence that, in furrow-type hypoplastic defects, a pronounced tapering of Retzius increments can occur, with the striae of Retzius forming acute angles with the outer enamel surface. We suggest that in such cases the outcrop of some striae of Retzius is essentially unobservable at the enamel surface, causing too low perikymata counts. The pronounced tapering of Retzius increments in outer enamel presumably reflects a mild to moderate disturbance of the function of late secretory ameloblasts. The implications of these findings for the reconstruction of crown growth patterns are discussed.

Dental enamel is formed in an incremental manner, and the rhythmic fluctuation in the activity of the secretory ameloblasts leaves a permanent record in the tissue. Incremental markings recordable in sectioned primate enamel include prism cross striations that reflect a circadian activity rhythm of the cells, and longer period markings in the form of striae of Retzius (Boyde, 1989; Hillson, 2014). The outcrops of the long period growth layers at the enamel surface are known as perikymata, with each perikyma consisting of a ridge, exhibiting a rather smooth surface with only very shallow Tomes' process pits, and a groove characterized by deeper Tomes' process pits . Typically, a stria of Retzius reaches the outer enamel surface (OES) at the bottom of a perikyma groove (Hillson, 2014). At the cervical margin of each perikyma groove, an increment margin marks the transition to the cervically adjacent perikyma. Thus, the enamel located between two consecutive increment margins at the OES corresponds to a Retzius increment, that is, the stretch of enamel between two consecutive striae of Retzius. In teeth with a known periodicity of the striae of Retzius (= repeat interval in days as evidenced by the number of prism cross striations), crown formation times of lateral (imbricational) enamel can be assessed based on perikymata counts. This approach has been widely used to reconstruct life history traits in extant and fossil hominoids (e.g. Reid et al., 2008; Smith, 2008; Dean, 2010; Hillson 2014) and to determine the timing of developmental stress events in great apes (Skinner and Hopwood, 2004; Guatelli-Steinberg et al., 2012; Skinner and Pruetz, 2012; Skinner 2014).

In a recent paper, Skinner and Pruetz (2012) reported the occurrence of a lower than expected number of perikymata between repetitive furrow-type hypoplastic enamel defects (defects of linear enamel hypoplasia, LEH) in a small number of chimpanzee (*Pan troglodytes verus*) canines from individuals of the Fongoli site in Senegal. The enamel defects were considered to have been caused by the repetitive negative impact on secretory ameloblast activity by the extended annual dry season occurring in this area. The number of perikymata expected to

occur between consecutive furrow-type defects in the canines of the Fongoli chimpanzees had been calculated by Skinner and Pruetz (2012) based on a typical stria of Retzius repeat interval of 6 or 7 days reported by Smith et al. (2007) in a large sample of common chimpanzee molars. Although higher repeat intervals of eight or nine have been recorded in chimpanzee enamel (Schwartz et al., 2001; Dean and Reid, 2001), the perikymata counts of Skinner and Pruetz (2012) would require a repeat interval of 10 to fit with the supposed annual occurrence of the environmental stress period considered causative for the observed furrow-type enamel defects. Such a high repeat interval has, however, so far not been recorded in chimpanzee enamel.

In their paper, Skinner and Pruetz (2012) put forward the hypothesis that a non-emergence of striae of Retzius in lateral (imbricational) enamel may be the cause for the lower than expected number of perikymata recorded between consecutive furrow-type defects in the Fongoli chimpanzee canines. This hypothesis was triggered by an observation on the locally flaked canine enamel of a male chimpanzee from the Taï Forest (Ivory Coast) population. In a cast of this tooth, Skinner and Pruetz (2012) observed a phenomenon in the exposed subsurface enamel that they described as presence of ‘minor striae’ between ‘major striae’. Both minor and major striae were regarded to reflect regular striae of Retzius. However, only the major striae were thought to be associated with a perikyma groove at the OES. In contrast, the minor striae were thought to peter out in outer enamel and therefore not to reach the OES. This would cause a difference between the number of Retzius increments deeper within the enamel layer and the number of perikymata recordable at the OES. Following this hypothesis, the existence of non-emergent striae could be an explanation for the ‘missing perikymata’ phenomenon and explain the too low number of perikymata observed between consecutive hypoplastic enamel defects thought to reflect an annually occurring drought period in the habitat of the Fongoli chimpanzees.

The hypothesis that in lateral (imbricational) enamel, some Retzius increments are regularly not associated with the presence of a perikyma at the OES is, however, at variance with our current understanding of enamel formation (see Hillson, (2014) for a recent review). Thus far, only in the case of severe, plane-type hypoplastic enamel defects of human teeth the presence of striae of Retzius whose outcrop at the OES was not recordable on external inspection has been reported (Gustafson, 1959; Witzel et al., 2008). This condition occurred in the ledge region positioned cervical to the exposed incremental plane and was caused by an extreme bending and convergence of striae of Retzius that formed a very acute angle with the OES.

A strong negative correlation between the total number of striae of Retzius and the stria of Retzius repeat interval has been reported for human canine enamel (Reid and Ferrell, 2006; McFarlane et al., 2014). In the study by Mc Farlane et al. (2014) it was further shown that the outcrop of each stria at the OES was associated with the presence of a distinct perikyma groove. This regular association allows a nondestructive estimation of the striae of Retzius repeat interval by counting perikymata in certain crown areas (McFarlane et al., 2014). Given these findings, and the conflicting hypothesis of non-emergent striae of Retzius (Skinner and Pruetz, 2012), it is of major importance to clarify whether or not in chimpanzee enamel the number of perikymata on the crown surface matches the number of Retzius increments within the enamel layer. This match is the prerequisite for a reliable reconstruction of the periodicity and duration of stress periods by inspection of crown surfaces (Skinner and Hopwood, 2004; Guatelli-Steinberg et al., 2012; Skinner and Pruetz, 2012; Skinner 2014).

The aims of the present study were, (1) to clarify the phenomenon of the so called non-emergent striae of Retzius in the enamel of chimpanzee canines, and (2) to provide additional data on crown formation parameters for canines of wild chimpanzees.

MATERIALS AND METHODS

The study was performed on three canines from three chimpanzees (*Pan troglodytes verus*). Two teeth originated from individuals of the Taï Forest population. The first of these specimens was the lower left canine of an adult male (Aramis, #15019, age not available). On a cast of this tooth, Skinner and Pruetz (2012) had made their original observation of 'non-emergent' striae of Retzius. The second specimen was the upper left canine of a young adult female (Zerlina, #11792, age 12.3 years). The number of perikymata in labial lateral (imbricational) enamel of this tooth had previously been established at 244 by Skinner et al. (2012). Neither of these chimpanzees was represented in the molar sample from the Taï Forest population previously studied by Smith et al. (2007). The third specimen was the lower right canine from the skull of a young adult (presumed female) individual (#Pan 15, former collection of the Department of Anthropology, University of Giessen, age not available) from East-Liberia collected in the 1950s or 1960s by H. Himmelheber. This skull, like the others collected by Himmelheber, was on display as a hunting trophy in the huts of a local ethnic group, the Dan (Schaefer, 1971). The skull is part of the Himmelheber collection now housed at the Senckenberg Natural History Museum in Frankfurt/Main, Germany

First, the crown surfaces of the three canines were inspected by either secondary electron imaging (Hitachi S 520 SEM, operated at 15 kV) or by backscattered electron (BSE) imaging in an FEI Quanta 600 FEG ESEM operated in a low-vacuum mode at an accelerating voltage of 20 kV. After obtaining the images of the crown surfaces, the teeth were embedded in epoxy resin (Biodur E12, Biodur products, Heidelberg, Germany) and subsequently sectioned in a labio-lingual direction using a rotary saw with a water-cooled diamond blade. In specimen #15019, the

section plane was positioned directly adjacent to the area of exposed subsurface enamel, where Skinner and Pruetz (2012) had made their observation of major and minor striae. In the other two specimens, the section planes ran through the highest point of the tooth crown.

For BSE imaging in the scanning-electron microscope (SEM), the cut surfaces were first smoothed with silicon sandpaper (grits 600 – 2,400) and then further polished on a motorized polisher (Labopol-5, Struers, Copenhagen, Denmark) with diamond suspensions of 3 and 1 µm particle diameter (DiaPro Dac 3 and 1, Struers). After obtaining the BSE images of the polished blocks, the polished surfaces were etched for 3 seconds with 5% phosphoric acid (v/v) thoroughly rinsed, dried, and again viewed in the FEI Quanta 600 FEG ESEM. Subsequently, the specimens were mounted with their polished sides down on glass slides. The mounted blocks were sectioned to a thickness of about 1 mm and then ground and polished to a final thickness of about 50 µm. The cover-slipped ground sections were viewed and photographed in transmitted light using an Axioskop 2Plus microscope (Zeiss, Jena, Germany). The acquired digital images were further processed using Adobe Photoshop CS4 (Adobe, San Jose, USA).

In the ground sections, the number of striae of Retzius were counted in labial lateral enamel. The stria of Retzius repeat interval (periodicity) was established by counting the number of prism cross striations between consecutive striae of Retzius. Daily enamel secretion rates (DSRs) were calculated in different crown regions (occlusal, upper-lateral, mid-coronal, upper-cervical) for the inner, central and outer thirds of the enamel layer, respectively. For this, the length of the prisms over five daily growth increments was measured in the central portions of the Retzius increments and divided by five, to produce a mean daily secretion rate. The values for the inner and outer enamel portion were measured at a minimum distance of 75 µm from the enamel-dentin-junction (EDJ) and the OES, respectively. Total crown formation time (CFT) was

calculated by adding the formation time of cuspal enamel to that of lateral enamel. Cuspal enamel formation time was calculated using a method (method B) described by Reid et al. (1998). All counts and measurements were made on single or stitched digital images using the Fiji freeware package with a stitching plugin (Preibisch et al., 2009).

RESULTS

Inspection of crown surfaces revealed that only in the canine of individual #11792 were enamel surface structures recordable over the entire crown surface, while in the other two specimens the enamel surface was abraded to an extent that precluded a recording of these traits. In enamel areas presenting mild or moderately developed furrow type defects, the enamel surface of the #11792 canine exhibited a variable spacing between clearly identifiable increment margins that were visible as meandering sharp lines (Fig. 1). In these areas, the enamel in places exhibited a surface structure that deviated from the normal situation. Typically, a perikyma exhibits an occlusally-located perikyma ridge with a rather smooth surface showing very shallow Tomes' process pits and a cervically adjacent perikyma groove with deeper Tomes' process pits. In contrast, in the enamel associated with the hypoplastic defects, a reverse pattern was present. Here a zone with rather deep Tomes' process pits was located occlusal to a zone with a relatively smooth surface (exhibiting only few and shallow Tomes' process pits) that bordered on the cervically adjacent increment margin (Fig. 1). At higher magnification, in places additional, less pronounced, horizontally running linear surface markings were visible between two distinct increment margins (Fig. 1b). These lesser markings were located at the occlusal border of the smooth-surfaced enamel.

BSE-SEM-images of the exposed subsurface enamel in the area where the surface enamel had flaked-off (canine of individual #15019) showed a more complex picture than previously reported by Skinner and Pruetz (2012). The exposed subsurface enamel was characterized by horizontally running steps separated by slightly inclined planes that partly exhibited a smooth surface (Fig. 2). The fracture surfaces forming the front of the steps showed a honeycomb-like pattern (Figs 2, 3a). Narrow clefts were present at the base of the step fronts (Fig. 2). These clefts are regarded to correspond to striae of Retzius exposed at the fracture plane. Thus, two consecutive clefts delimit a Retzius increment. The upper rims of the step fronts were prominent and corresponded to the 'major striae' described by Skinner and Pruetz (2012). The inclined planes located between consecutive honeycombed fracture faces often exhibited a secondary fracture step of lower height (Fig. 2). The fracture fronts of these secondary steps showed either no, or an indistinct, honeycomb pattern (Fig. 3a).

BSE-SEM images of the labio-lingual section of the #15019 canine revealed a characteristic structure of the subsurface enamel (Fig. 3b,c). Within an individual Retzius increment, the enamel externally adjacent to a stria of Retzius was typically aprismatic over a certain distance, and only the more peripherally located enamel within this increment showed a prismatic structure (Fig. 3b,c). The relative extension of the zone of aprismatic enamel within a Retzius increment increased towards the OES and was therefore greatest in outermost enamel, where it sometimes constituted the entire increment (Fig. 3c).

The topography of the exposed fracture plane shown in figures 2 and 3a can be related to the described structural variation of the outer enamel (Fig. 3b,c). Thus, the honeycombed fracture face corresponds to a fracture surface of prismatic enamel, with the transversely fractured prisms surrounded by interprismatic enamel. The honeycombed fracture faces are located approximately

at the level of the striae of Retzius planes (Fig. 3b,c) that apparently constitute zones of weakness. The inclined planes located between the honeycombed fracture faces constitute fracture faces running more or less parallel to the long axis of the enamel prisms (Fig. 3b,c). The secondary fracture steps occurring in these planes are deemed to be caused by the transition between the (inner) aprismatic and the (outer) prismatic enamel portion within an individual Retzius increment (Fig. 3b,c). In our view, the 'minor striae' reported by Skinner and Pruetz (2012) correspond to these secondary steps in the fracture surface.

An additional observation made in sections of the studied canines was an extreme tapering of single or multiple Retzius increments and a concurrent convergence of the striae of Retzius in the outer enamel of crown areas exhibiting furrow-type hypoplastic defects (Figs 3b, 4). In these areas, the striae of Retzius ran more or less tangentially to the OES and formed extremely acute angles with the enamel surface. The surface enamel was mostly aprismatic in such locations and the Retzius increment tapered out into an extremely thin sheet of enamel that at the OES partly overlapped the occlusally adjacent Retzius increment (Figs 3b, 4a). It is assumed that in such cases the outcrop of some striae of Retzius at the OES is not discernible by inspection of the crown surface at lower magnifications. However, the microscopic analyzes clearly demonstrated that all striae of Retzius reached the OES (Figs 4a,b).

The recorded DSRs for the different crown regions of the three studied canines are given in table 1. In all specimens, a tendency for an increase in DSRs from the inner over the central towards the outer enamel was observed. Mean DSRs ranged between 2.94 µm/day in inner upper cervical enamel (individual #15019) and 5.19 µm/day in outer occlusal enamel (individual #Pan 15). Stria of Retzius repeat intervals were nine in individual #11792 (Fig. 5) and eight in individual #Pan 15 and individual #15019. Repetitive counts of the total number of striae of

Retzius in labial, lateral enamel by two of the authors (CW, HK) revealed mean numbers of 251 in #11792, of 281 in #Pan 15 and of 295 in #15019 (values of individual counts did not vary by more than 2). Based on the reported repeat intervals, total CFTs (lateral + cuspal enamel formation times) were calculated at 6.84 years (#Pan 15), 6.87 years (#11792), and 7.32 years (#15019).

DISCUSSION

Our results on the canine of #15019 do not support the hypothesis of Skinner and Pruetz, (2012) of the occurrence of non-emergent striae of Retzius as the cause underlying the 'too low' perikymata counts in the Fongoli chimpanzees. Based on our observations, we conclude that the (non-emergent) 'minor striae' described by these authors can be attributed to variations in enamel structure and a resulting differential fracture behavior of the outer enamel. In this enamel zone, individual Retzius increments comprise a zone of aprismatic enamel external to a stria of Retzius and a zone of prismatic enamel further peripherally. This is regarded to reflect the fact that in late secretory ameloblasts, the recovery to full secretory activity and the concomitant re-establishment of a fully developed Tomes' process, required for formation of prismatic enamel (Boyde 1989; Kierdorf and Kierdorf, 1997; Witzel et al., 2008), is delayed following the occurrence of a stria of Retzius. In our interpretation, the 'minor striae' of Skinner and Pruetz (2012) constitute fracture faces formed at the transition between aprismatic enamel and prismatic enamel within a Retzius increment. Variation in the timing of the recovery of full secretory activity by late secretory ameloblasts and thus the onset of prism formation can cause variation in the position of these minor (secondary) steps.

Our findings, however, also provide evidence that under certain conditions some Retzius increments will not be recordable as perikymata at the crown surface. Thus, in crown areas showing furrow-type hypoplastic defects, a pronounced tapering of Retzius increments was observed with the striae of Retzius forming acute angles with the OES. The enamel in these areas is largely aprismatic. We assume that in these cases, the outcrop of the striae of Retzius at the OES is not discernible on external inspection using routine methods such as the inspections of casts at lower magnifications (50 to 100 x). This will result in a 'too low' perikymata count. However, when studying the original enamel surface at higher magnification in the SEM, the outcrop of these striae of Retzius at the OES may, at least in places, be observable (see Fig. 1b). The extreme tapering of Retzius increments near the OES presumably reflects a mild to moderate impact on the late secretory ameloblasts with the number of affected Retzius increments indicating the duration of the stress period.

The fact that in the labial lateral enamel of the #11792 canine only 244 perikymata were counted (Skinner et al., 2012), while our histological analysis revealed the presence of 251 striae of Retzius is considered to reflect the fact that striae of Retzius forming an extremely acute angle with the OES do not leave a trace at the enamel surface recordable at lower magnification. This condition may be the cause for the variable spacing between recognizable increment margins and the abnormally wide 'atypical perikymata' observed in areas of the crown as shown in figure 1. The areas with a rather smooth surface structure present adjacent to the cervically located increment margins may be caused by the presence of thin sheets of aprismatic enamel in the outermost zone of extremely tapered Retzius increments that partly overlap the occlusally located Retzius increment. It is suggested that in such cases the stretch of surface enamel between two recognizable successive increment margins, which would be recorded as a single, enlarged 'perikyma' on external inspection (see figure 1) equals more than one long period (Retzius)

increment. In the case of the canine of individual #11792 the lower perikymata count compared to the stria of Retzius count in labial lateral enamel leads to a difference of approximately two months between the two estimates for the formation of this enamel portion.

Although a direct comparison between the increment pattern at the enamel surface and that within the enamel was not possible in the other two specimens, the histological findings indicate the presence of a similar situation also in the canines of #15019 and #Pan 15. Thus, our data provide evidence that in chimpanzee canines exhibiting furrow-type hypoplastic enamel defects, a 'missing perikymata' phenomenon can exist. This condition reflects a temporary impairment of the function of late secretory ameloblasts and thus differs in both its causation and the frequency of its occurrence from the phenomenon originally hypothesized to occur in chimpanzee canines by Skinner and Pruetz (2012).

The influence of the angles formed between the striae of Retzius and the OES on the expression and visibility of enamel surface structures was previously also demonstrated by Guatelli-Steinberg et al. (2012) in a study on the occurrence of linear enamel hypoplasia in great apes. These authors showed that when striae of Retzius formed angles of less than 20 to 30 degrees with the enamel surface, furrow-type hypoplastic defects were broad and shallow and therefore difficult to identify by surface inspection. Guatelli-Steinberg et al. (2012) concluded that in great ape enamel, regularly occurring differences in the angles between striae of Retzius and the OES contribute consistently to the reported variation in the frequency of LEH among the different great ape species.

Our histological analysis revealed repeat intervals of eight or nine in the studied chimpanzee canines. Although periodicities of 8 or 9 have previously been reported in the enamel of *Pan troglodytes* (Reid et al., 1998; Dean and Reid, 2001; Schwartz et al., 2001) and *Pan*

paniscus (Ramirez Rozzi and Lacruz, 2007), by far the most frequent periodicities recorded in chimpanzee enamel are six and seven (Schwartz et al., 2001, Smith et al. 2007). Our findings caution against an uncritical adoption of this 6 or 7 day periodicity for calculating CFTs in chimpanzees (with unknown enamel periodicity) because this may mask the variation present within and among populations. As it is not always feasible to perform time-consuming histological analysis on chimpanzee teeth, and destructive analysis is often not possible in this material, the method used by McFarlane et al. (2014) for human canines may be useful also for a nondestructive assessment of repeat intervals and CFTs in chimpanzee teeth. It must however be considered that, contrary to the findings in human canines (Reid and Ferrell, 2006; McFarlane et al., 2014), Smith et al. (2007) in their study on chimpanzee molars found no consistent relationship between striae of Retzius periodicity and the total number of striae of Retzius. Further studies on the relationship between the number of striae of Retzius and the repeat interval in chimpanzee enamel are needed to resolve this issue.

Calculated CFTs for the studied chimpanzee canines (6.84 years in individual #Pan 15; 6.87 years in individual #11792, and 7.32 years in individual #15019) are within the range of those previously reported for *Pan troglodytes* canines. Based on histological analysis, Reid et al. (1998) reported a CFT of 7.03 years (recalculated from table 4 of Reid et al., 1998) in the lower canine of an adult female and of 7.14 years in the (still incomplete) upper canine of a juvenile of unknown sex. Schwartz and Dean (2001), likewise using histological analysis, reported mean CFTs of 6.81 ± 0.56 years (SD) (range: 5.91 – 7.58 years) for mandibular canines of male chimpanzees, and of 5.85 ± 0.51 (SD) years (range: 5.28 – 6.49 years) in females. In a radiographic study, Kuykendall (1996) reported mean CFTs (recalculated from table 3 of Kuykendall, 1996) of mandibular canines of 6.83 years (range: 5.92 – 7.75 years) in male (n = 2) and of 5.97 years (range: 5.12 – 7.21 years) in female (n = 8) chimpanzees.

DSRs recorded in the three canines analyzed by us increased from the inner to the outer enamel. This is in line with previous findings in molar and canine enamel of common chimpanzees (Dean, 1998; Reid et al., 1998; Schwartz et al., 2001; Smith et al., 2007). DSRs recorded in the present study are similar to those previously reported for chimpanzee enamel. Thus, Reid et al. (1998) found mean DSRs between 2.89 μm/day in inner and 4.68 μm/day in outer enamel of mandibular canines and between 3.10 μm/day in inner and 4.93 μm/day in outer enamel of maxillary canines. In the inner enamel of mandibular canines, Schwartz et al. (2001) recorded mean DSRs between 2.66 and 3.37 μm/day, while DSR values in outer enamel ranged between 3.74 and 4.39 μm/day. DSRs in molar enamel of *Pan troglodytes* have been reported to vary between 2.6 to 2.8 μm/day in inner and approximately 5.8 μm/day in outer enamel (Dean, 1998; Smith et al., 2007).

In conclusion, the present study provided evidence that in chimpanzee canines affected by furrow- type enamel hypoplasia, some Retzius increments are not associated with perikymata visible on routine (low magnification) external inspection of the crown surface. This can cause a certain underestimation of lateral enamel formation time based on perikymata counts. However, a non-emergence of striae of Retzius in chimpanzee canines, as was previously surmised by Skinner and Pruetz (2012) was not confirmed in the present study. The high repeat intervals recorded in the enamel of the studied canines caution against a general adoption of a striae of Retzius repeat interval of 6 or 7 days for the enamel of common chimpanzees as this may cause an erroneous underestimation of CTFs and the periodicity of repetitive furrow-type (LEH) enamel defects.

LITERATURE CITED

Boyde A. 1989. Enamel. In: Oksche A, Vollrath L (editors). Teeth. Handbook of Microscopic Anatomy Vol. V/6. Berlin: Springer. p. 309-473.

Dean MC. 1998. A comparative study of cross striation spacings in cuspal enamel and four methods of estimating the time taken to grow molar cuspal enamel in *Pan*, *Pongo* and *Homo*. J Hum Evol 35:449-462.

Dean MC. 2010. Retrieving chronological age from dental remains of early fossil hominins to reconstruct human growth in the past. Phil Trans R Soc B 365:3397-3410.

Dean C, Reid DJ. 2001. Perikymata spacing and distribution on hominoid anterior teeth. Am J Phys Anthropol 116:209-215.

Guatelli-Steinberg D, Ferrell RJ, Spence J. 2012. Linear enamel hypoplasia as an indicator of physiological stress in great apes: Reviewing the evidence in light of enamel growth variation. Am J. Phys Anthropol 148:191-204.

Gustafson AG. 1959. A morphologic investigation of certain variations in the structure and mineralization of human dental enamel. Odont. Tidskr 67:361-472.

Hillson S. 2014. Tooth development in human evolution and bioarchaeology. Cambridge. Cambridge University Press.

Kierdorf H, Kierdorf U. 1997. Disturbances of the secretory stage of amelogenesis in fluorosed deer teeth: a scanning electron-microscopic study. Cell Tissue Res 289:125-135.

Kuykendall KL. 1996. Dental development in chimpanzees (*Pan troglodytes*): the timing of calcification stages. Am J Phys Anthropol 99:135-157.

McFarlane G, Littleton J, Floyd B. 2014. Estimating striae of Retzius periodicity nondestructively using partial counts of perikymata. Am J Phys Anthropol 154:251-258.

Preibisch S, Saalfeld S, TomancekP. 2009. Globally optimal stitching of tilted 3D microscopic image acquisitions. Bioinformatics 25:1463-1465.

Ramirez Rozzi F., Lacruz RS. 2007. Histological study of an upper incisor and molar of a bonobo (*Pan paniscus*) individual. In: Bailes SE, Hublin J-J, editors. Dental perspectives on human evolution. Dordrecht: Springer. p. 163-176.

Reid DJ, Ferrell RJ. 2006. The relationship between number of striae of Retzius and their periodicity in imbricational enamel formation. J Hum Evol 50:195-202.

Reid DJ, Guatelli-Steinberg D, Walton P. 2008. Variation in modern human premolar enamel formation times: Implications for Neandertals. J Hum Evol 54:225-235.

Reid DJ, Schwartz GT, Dean C, Chandrasekera MS. 1998. A histological reconstruction of dental development in the common chimpanzee, *Pan troglodytes*. J Hum Evol 35:427-448.

Schaefer, U. 1971. Künstliche Eröffnung des Foramen occipitale magnum bei Vormenschen und rezenten Schimpansen. Anthrop Anz 33:109-113.

Schwartz GT, Dean C. 2001. Ontogeny of canine dimorphism in extant hominoids. Am J Phys Anthropol 115:269-283.

Schwartz GT, Reid DJ, Dean C. 2001. Developmental aspects of sexual dimorphism in hominoid canines. Int J Primatol 22:837-860.

Skinner MF. 2014. Variation in perikymata counts between repetitive episodes of linear enamel hypoplasia among orangutans from Sumatra and Borneo. Am J Phys Anthropol 154:125-139.

Skinner MF, Hopwood D. 2004. Hypothesis for the causes and periodicity of repetitive linear enamel hypoplasia in large, wild African (*Pan troglodytes* and *Gorilla gorilla*) and Asian (*Pongo pygmaeus*) apes. Am J Phys Anthropol 123:216-235.

Skinner MF, Pruetz JD. 2012. Reconstruction of periodicity of repetitive linear enamel hypoplasia from perikymata counts on imbricational enamel among dry-adapted chimpanzees (*Pan troglodytes verus*) from Fongoli, Senegal. Am J Phys Anthropol 149:468-482.

Skinner MF, Skinner MM, Boesch C. 2012. Developmental defects of the dental crown in chimpanzees from the Taï National Park, Côte D'Ivore: Coronal waisting. Am J Phys Anthropol 149:272-282.

Smith TM. 2008. Incremental dental development: Methods and applications in hominoid evolutionary studies. J Hum Evol 54:205-224.

Smith TM, Reid DJ, Dean MC, Olejniczak AJ, Martin LB. 2007. Molar development in common chimpanzees (*Pan troglodytes*). J Hum Evol 52:201-216.

Witzel C, Kierdorf U, Schultz M, Kierdorf H. 2008. Insights from the inside: Histological analysis of abnormal enamel microstructure associated with hypoplastic defects in human teeth. Am J. Phys Anthropol 136:400-414

Figure legends

Fig.1. SEM-BSE images of uncoated labial-cervical enamel surface of upper left canine of individual #11792. **(a)** Perikymata with normal appearance are marked by white double-headed arrows. 'Atypical perikymata' are marked by black double-headed arrows. The latter are located in the area of a furrow-type hypoplastic defect. Note presence of a smooth surface zone located cervically within these 'atypical perikymata'. **(b)** Higher magnification of 'atypical perikymata' in the hypoplastic defect area. Arrowheads: clearly visible increment margins. Arrows: Faintly visible linear surface markings interpreted as less pronounced increment margins. Asterisks: smooth surface zone in the cervical portion of an 'atypical perikyma'. Occlusal to top of images.

Fig.2. SEM-BSE image of step-like fracture plane in subsurface enamel of the lower left canine of individual #15019. White arrows: clefts corresponding to the openings of striae of Retzius at the fracture plane. Black arrowheads: upper rims of major steps in the fracture plane that themselves exhibit a honeycomb-like pattern. Asterisks: secondary steps in the fracture plane. Occlusal to top of image.

Fig. 3. SEM-BSE images of exposed fracture plane **(a)** and labio-lingually oriented sections though labial enamel **(b, c)** of the lower left canine of individual #15019. **(a)** White brackets mark major steps in the fracture surface. Black bracket: secondary step in the fracture surface located at the transition between prismatic and aprismatic enamel. White double-headed arrow: fracture face oriented along the prism long axes. Black double-headed arrow: inclined fracture plane in aprismatic enamel. In **(b)** and **(c)** the structures of intact outer enamel that correspond to

those identified in the fracture surface are marked with the same symbols as in **(a)**. Arrowhead in **(b)**: Pronounced tapering of a Retzius increment. Occlusal to top of images.

Fig. 4. Sectioned outer labial enamel of upper left canine of individual #11792 **(a),** and lower right canine of individual #Pan 15 **(b)**. **(a)** SEM-BSE image showing extreme tapering of successive Retzius increments. Arrowheads mark the opening of three consecutive striae of Retzius at the OES. Openings number 1 and 3 are most likely not recordable on routine (low magnification) inspection of the enamel surface. Arrow: deepest point of OES that does not correspond to the opening of a stria of Retzius. Asterisks: striae of Retzius. **(b)** Ground section viewed in transmitted light with phase-contrast. Note extreme tapering (arrowheads) of successive Retzius increments and concomitant bending of striae of Retzius. Arrow indicates prism direction. Occlusal to top of images.

Fig. 5. Striae of Retzius periodicity of nine illustrated in prismatic **(a)** and aprismatic **(b)** labial enamel of the upper left canine of individual #11792. **(a)** labio-lingually oriented ground section viewed in transmitted light with phase contrast. Arrows: striae of Retzius. Dots: daily growth marks. **(b)** SEM-BSE image of labio-lingually oriented section. Arrows: striae of Retzius. Dots: daily growth marks in aprismatic enamel. Occlusal to top of images.

TABLE 1. Mean daily secretion rates (± standard deviations) (µm/day) in inner, central and outer enamel of upper (individual #11792) and lower (individuals #Pan 15 and #15019) canines from three chimpanzees at different locations along the vertical tooth axis. Numbers in brackets indicate the number of measurements included in the respective mean.

Individual/location	occlusal	upper lateral	midcoronal	upper cervical
#11792/inner	3.50 ± 0.38 (28)	3.79 ± 0.41 (21)	3.45 ± 0.32 (28)	3.37 ± 0.34 (30)
#11792/central	4.37 ± 0.34 (25)	4.60 ± 0.44 (22)	4.30 ± 0.29 (26)	3.96 ± 0.36 (27)
#11792/outer	4.79 ± 0.44 (22)	4.59 ± 0.40 (23)	4.50 ± 0.43 (33)	4.03 ± 0.28 (33)
#Pan 15/inner	3.90 ± 0.53 (25)	3.87 ± 0.33 (25)	3.07 ± 0.39 (27)	3.32 ± 0.35 (25)
#Pan15/central	4.56 ± 0.59 (24)	4.52 ± 0.34 (25)	3.52 ± 0.50 (25)	3.84 ± 0.26 (25)
#Pan 15/outer	5.19 ± 0.56 (25)	4.53 ± 0.42 (25)	4.15 ± 0.40 (24)	3.99 ± 0.43 (25)
#15019/inner	3.64 ± 0.39 (27)	3.82 ± 0.39 (21)	3.83 ± 0.30 (25)	2.94 ± 0.25 (24)
#15019/central	4.32 ± 0.36 (21)	4.67 ± 0.26 (23)	4.39 ± 0.34 (26)	3.72 ± 0.25 (26)
#15019/outer	4.65 ± 0.41 (26)	4.63 ± 0.28 (22)	4.39 ± 0.28 (26)	3.83 ± 0.22 (25)

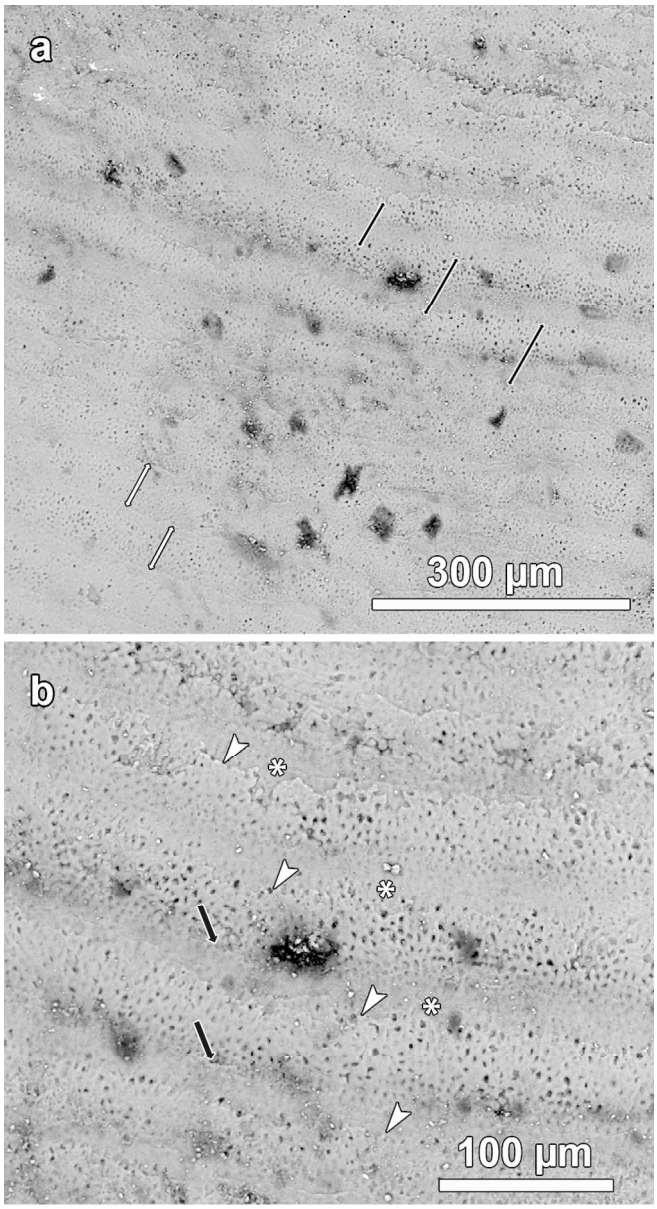

Fig.1. SEM-BSE images of uncoated labial-cervical enamel surface of upper left canine of individual #11792. (a) Perikymata with normal appearance are marked by white double-headed arrows. 'Atypical perikymata' are marked by black double-headed arrows. The latter are located in the area of a furrow-type hypoplastic defect. Note presence of a smooth surface zone located cervically within these 'atypical perikymata'. (b) Higher magnification of 'atypical perikymata' in the hypoplastic defect area. Arrowheads: clearly visible increment margins. Arrows: Faintly visible linear surface markings interpreted as less pronounced increment margins. Asterisks: smooth surface zone in the cervical portion of an 'atypical perikyma'. Occlusal to top of images.
80x147mm (300 x 300 DPI)

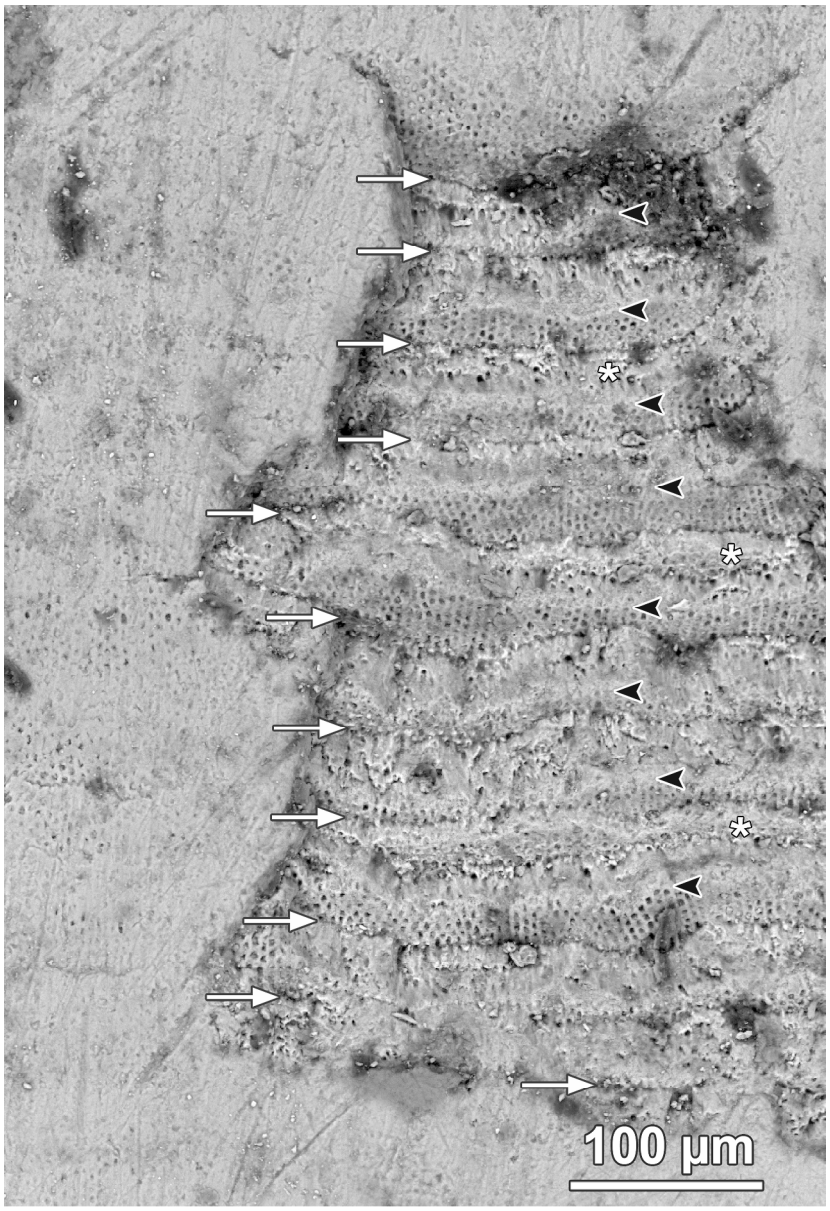

Fig.2. SEM-BSE image of step-like fracture plane in subsurface enamel of the lower left canine of individual #15019. White arrows: clefts corresponding to the openings of striae of Retzius at the fracture plane. Black arrowheads: upper rims of major steps in the fracture plane that themselves exhibit a honeycomb-like pattern. Asterisks: secondary steps in the fracture plane. Occlusal to top of image.

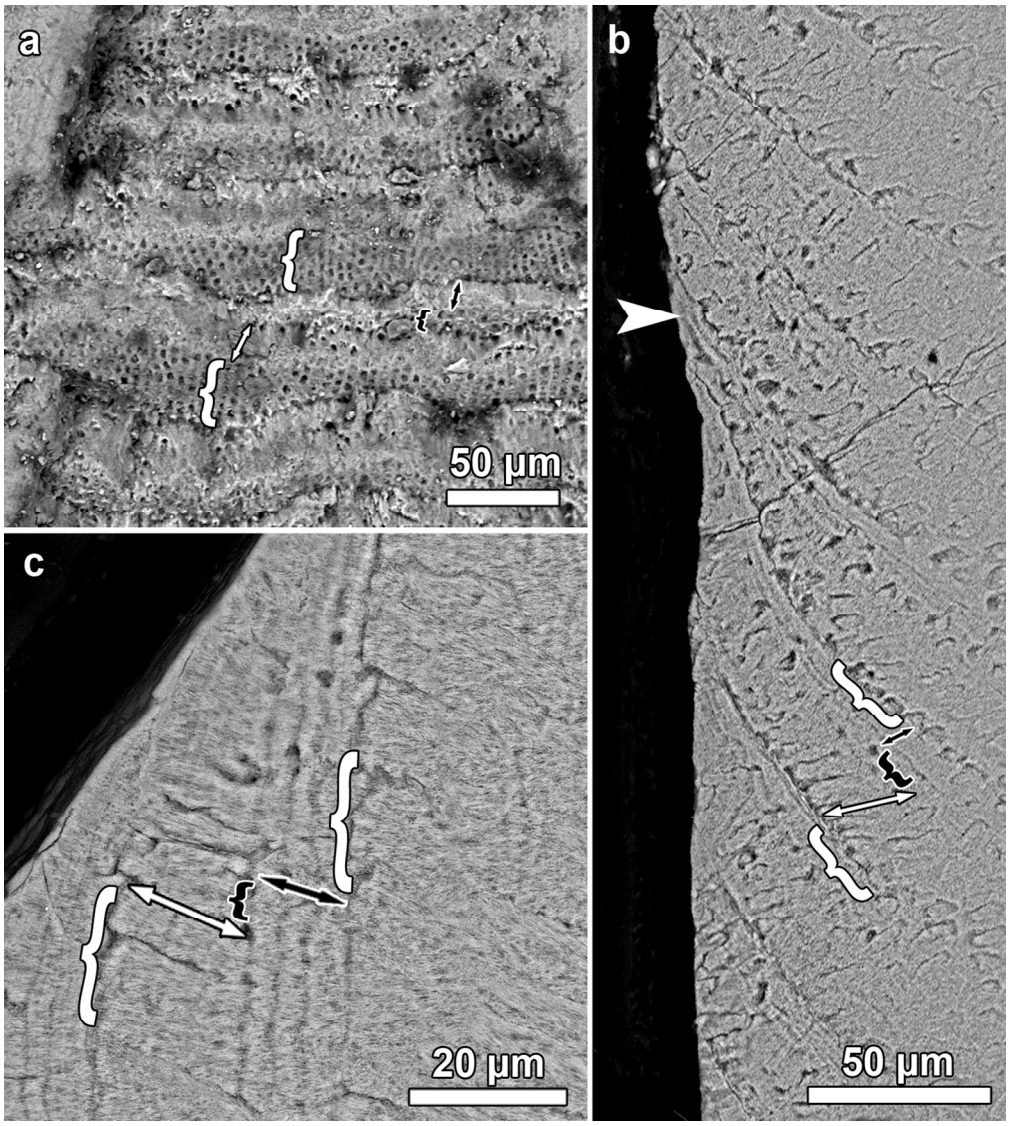

Fig. 3. SEM-BSE images of exposed fracture plane (a) and labio-lingually oriented sections though labial enamel (b, c) of the lower left canine of individual #15019. (a) White brackets mark major steps in the fracture surface. Black bracket: secondary step in the fracture surface located at the transition between prismatic and aprismatic enamel. White double-headed arrow: fracture face oriented along the prism long axes. Black double-headed arrow: inclined fracture plane in aprismatic enamel. In (b) and (c) the structures of intact outer enamel that correspond to those identified in the fracture surface are marked with the same symbols as in (a). Arrowhead in (b): Pronounced tapering of a Retzius increment. Occlusal to top of images.
124x139mm (300 x 300 DPI)

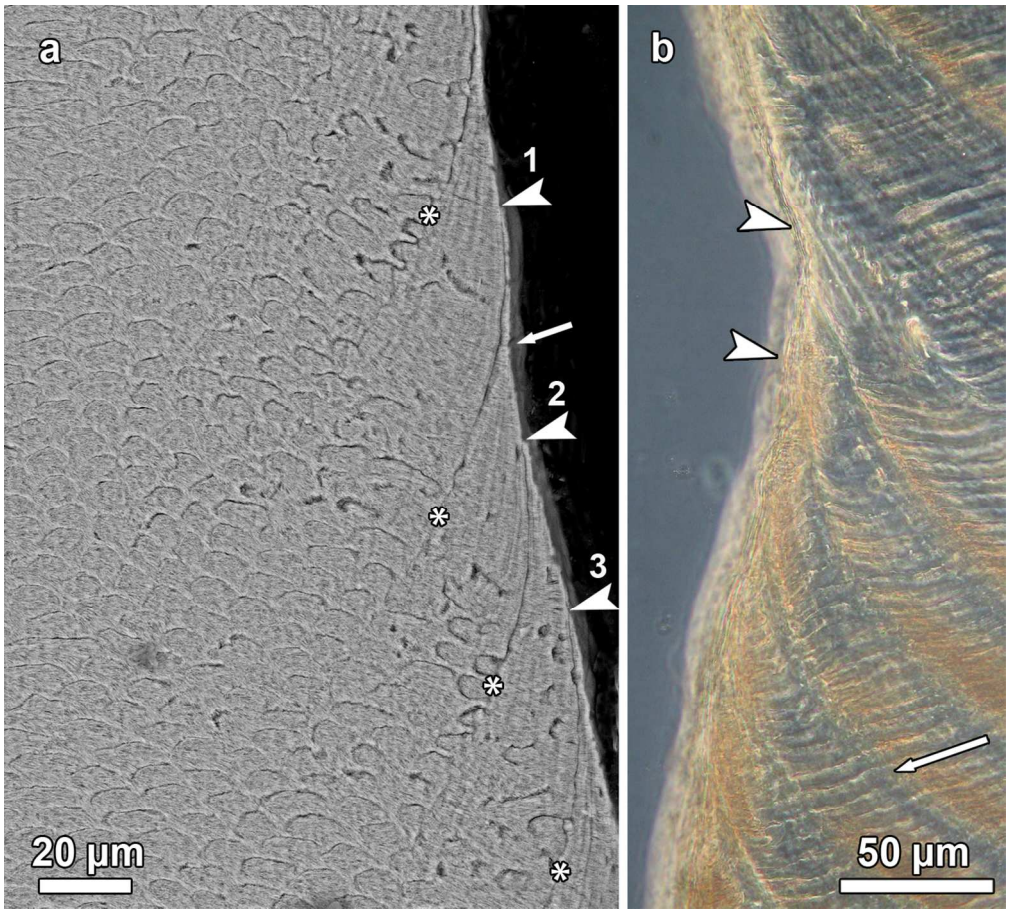

Fig. 4. Sectioned outer labial enamel of upper left canine of individual #11792 (a), and lower right canine of individual #Pan 15 (b). (a) SEM-BSE image showing extreme tapering of successive Retzius increments. Arrowheads mark the opening of three consecutive striae of Retzius at the OES. Openings number 1 and 3 are most likely not recordable on routine (low magnification) inspection of the enamel surface. Arrow: deepest point of OES that does not correspond to the opening of a stria of Retzius. Asterisks: striae of Retzius. (b) Ground section viewed in transmitted light with phase-contrast. Note extreme tapering (arrowheads) of successive Retzius increments and concomitant bending of striae of Retzius. Arrow indicates prism direction. Occlusal to top of images.
124x112mm (300 x 300 DPI)

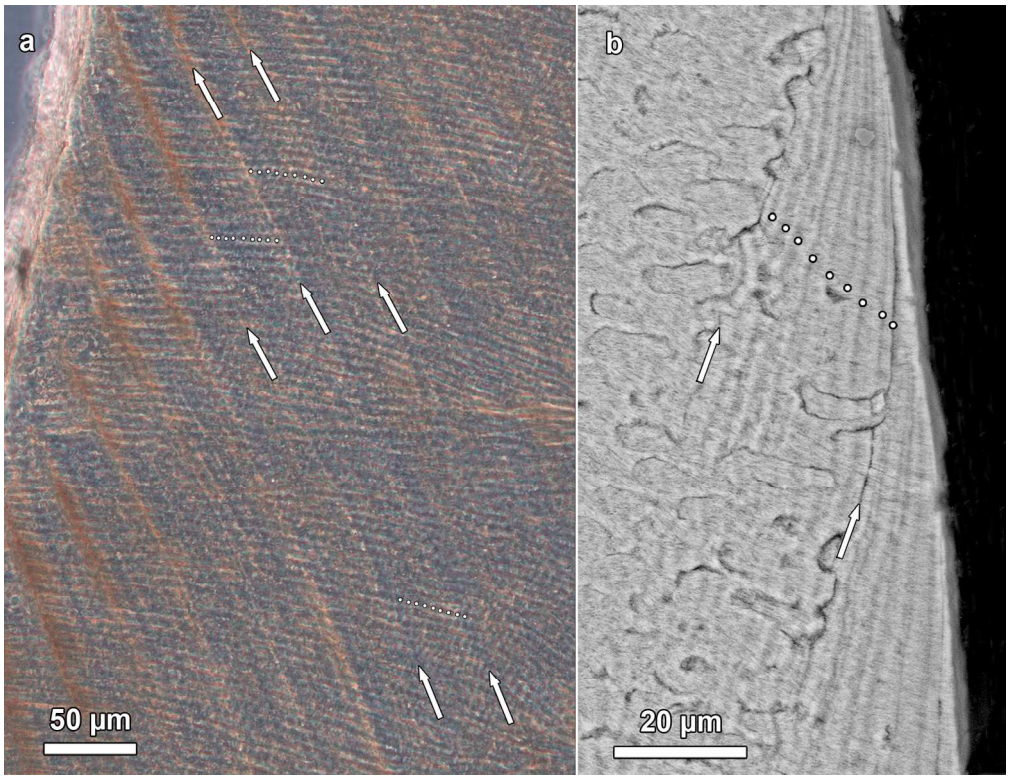

Fig. 5. Striae of Retzius periodicity of nine illustrated in prismatic (a) and aprismatic (b) labial enamel of the upper left canine of individual #11792. (a) labio-lingually oriented ground section viewed in transmitted light with phase contrast. Arrows: striae of Retzius. Dots: daily growth marks. (b) SEM-BSE image of labio-lingually oriented section. Arrows: striae of Retzius. Dots: daily growth marks in aprismatic enamel. Occlusal to top of images.
171x132mm (300 x 300 DPI)